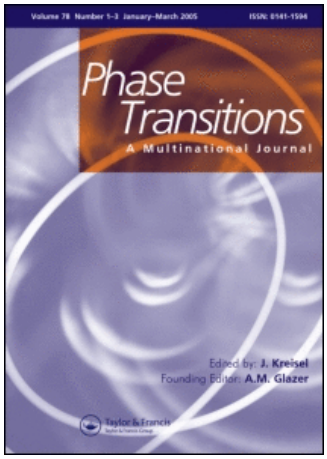

Phase Transitions
A Multinational Journal
Publication details, including instructions for authors and subscription information:
http://www.informaworld.com/smpp/title~content=t713647403

Proton conductivity and ferroelectric phase transition in hydrogen-bonded ferroelectric NH_4IO_3

M. M. Abdel-Kader [a]; F. El-Kabbany [a]; H. Naguib [a]; W. M. Gamal [a]
[a] Faculty of Science, Department of Physics, Cairo University, Giza, Egypt

Online Publication Date: 01 January 2008
To cite this Article: Abdel-Kader, M. M., El-Kabbany, F., Naguib, H. and Gamal, W. M. (2008) 'Proton conductivity and ferroelectric phase transition in hydrogen-bonded ferroelectric NH_4IO_3', Phase Transitions, 81:1, 83 - 99
To link to this article: DOI: 10.1080/01411590701586936
URL: http://dx.doi.org/10.1080/01411590701586936

Phase Transitions,
Vol. 81, No. 1, January 2008, 83–99

Proton conductivity and ferroelectric phase transition in hydrogen-bonded ferroelectric NH_4IO_3

M. M. ABDEL-KADER*, F. EL-KABBANY,
H. NAGUIB and W. M. GAMAL

Faculty of Science, Department of Physics, Cairo University, Giza, Egypt

(*Received 13 July 2007; accepted 22 July 2007*)

We report on the ac dielectric permittivity (ε) and the electric conductivity (σ_ω), as function of the temperature $300\,\mathrm{K} < T < 400\,\mathrm{K}$ and frequency 0.5–100 kHz for polycrystalline samples of hydrogen-bonded ferroelectric ammonium iodate, NH_4IO_3. The main feature of our measured parameters is that, the compound undergoes a ferroelectric phase transition of an improper character, at (368 ± 1)K from a high temperature paraelectric phase I ($Pm2_1b$) to a low temperature ferroelectric phase II ($Pc21n$). The electric conduction seems to be protonic. The frequency dependent conductivity has a linear response following the universal power law ($\sigma_{(\omega)} = A(T)\omega^{s(T)}$). The temperature dependence of the frequency exponent s suggests the existence of two types of conduction mechanisms.

Keywords: Phase transition; Ammonium iodate, NH_4IO_3; Proton conductivity; Improper ferroelectric

1. Introduction

Proton conduction in solids via hydrogen bonding was first suggested by Ubbelohde and Rogers [1] and was developed later on, to explain the conductivity of the paraelectric phase of potassium hydrogen phosphate, KH_2PO_4 (KDP) [2]. Currently, proton conductors appear interesting because of protonic transport in biophysical processes – as with many other ionic conductors – since they can be used in numerous electrochemical devices such as batteries, fuel cells, chemical sensors, electrochromic displays and supercapacitors [3]. Furthermore, energy systems based on hydrogen give a possible answer to prevent earth pollution. Proton conductivity is a particular case of ionic conduction. However, the small dimensions of the proton implies that there may be some similarities with electronic conduction. Obviously, the hydrogen bonding is a pre-request for proton conduction.

Ammonium iodate, NH_4IO_3, seems to be a candidate for such protonic conductors, since the molecules of the compound are hydrogen-bonded in their crystalline state. Furthermore, the compound is a member of the iodate series of the

*Corresponding author. Email: m_m_abdelkader@yahoo.com

Phase Transitions
ISSN 0141-1594 print/ISSN 1029-0338 online © 2008 Taylor & Francis
http://www.tandf.co.uk/journals
DOI: 10.1080/01411590701586936

general molecular formula MIO_3 where M is a monovalent element and/or group [M = H, Li, Na, K, Rb, Cs, Tl and NH_4]. Each of these materials is a centric, with large indices of refraction [4]. Some members of these series undergo successive phase transitions at low and high temperatures [5]. Some of these phases are ferroelectrics and/or ferroelastics [6]. Compound with $M = NH_4$, is the most interesting member of this series because it is the only one that contains the NH_4 group which is the main source of the hydrogen bonding, in addition to the usual IO_3 group, which is also participating in the hydrogen bonding system. The room temperature crystal structure of NH_4IO_3 single crystals was determined by using X-ray diffraction technique [4]. The data indicated that, the compound crystallizes in the orthorhombic system with space group $Pc2_1n$ and four formulae in the unit cell. The lattice constants are:

$$a = 6.4115, b = 9.1706 \quad \text{and} \quad c = 6.3740\text{A}.$$

Like other ammonium compounds, the NH_4IO_3 attracts the attention of investigators over the past several years. Preliminary report on the optical refractive indices and pyroelectric current was given by Crane *et al.* [7]. The report indicated that the NH_4IO_3 is a nonlinear optical material and the crystal is piezoelectric along all the three axes. Furthermore, their results clarified the existence of a phase transition initiated at 85°C (358 K) and completed around ≈90°C (363 K), where the crystal was changed from a polar, pyroelectric phase to a piezoelectric non-polar phase.

Regarding the ferroelectricity in the NH_4IO_3, it is known that Oka *et al.* [8] reported the first observation of the polarity reversal by the dc electric field and therefore, they demonstrated the existence of ferroelectricity in this compound. Thus, the NH_4IO_3 is known since then to be ferroelectric from that date onwards. The first report on the ferroelasticity of this compound was given by Abrahams and Keve [4], their results indicated that the compound is potentially ferroelastic with a spontaneous strain of about 0.00293 at room temperature.

An earlier report on the lattice dynamics and Raman spectroscopy of this compound was given by Salje [9]. Furthermore, the phase transformation was investigated by optical, X-rays and Raman spectroscopic techniques at different temperatures and pressures [10]. The temperature of transformation as determined, while probe was heated, varied between 360 and 368 K for different crystals, but all probes showed the same temperature (355 ± 2 K) on cooling. Another phase transformation was also observed at ≈388 K. The temperature dependence of the electro-optical effect and the double refraction as studied by Salje *et al.* [11], suggested the existence of two phase transitions at ≈355.5 and 393 K.

The mechanism of the structural transformation in the NH_4IO_3 single crystals and the detail of the crystal structure of the high temperature phase (above 83°C, according to this study), were described by Bismayer *et al.* [12]. Their data showed that, the high temperature phase is also orthorhombic, space group $Pm2_1b$ and with lattice constants: $a = 6.426$Å, $b = 9.104$ Å and $c = 6.466$Å. Furthermore, the effect of the hydrostatic pressure on the ferroelectric transition temperature was investigated by Shimizu *et al.* [13].

Relatively, recent series of papers [14, 15] dealing with vibration spectra (IR, Raman and 127_I NQR spectra) for single crystals of NH_4IO_3 in the temperature

range 300–400 K, confirmed the existence of a ferroelectric phase transition with a Curie temperature $Tc = 367$ K. No structural phase changes at $\approx$355.5 K and in the region $\approx$ (388–393 K) as proposed by Salje *et al.* [10, 11] have been detected using the same measuring technique.

Ammonium iodate belongs to an interesting class of compounds known as hydrogen-bonded ferroelectrics. The best known example of this family is the KDP. Compounds which behave like KDP are termed as KDP-type ferroelectrics. Although the hydrogen-bonded ferroelectrics have been extensively studied they are still of interest because of the continuing controversy over the nature of the phase transitions in addition to their technological importance [16].

In a recent article [17] a new technique, namely, a magnetic probe (muon), was used for studying the dynamics of hydrogen-bonded ferroelectric and antiferroelectric phenomena. Moreover, a new series of trivalent metallic iodates of a general molecular formula $M(IO_3)_3$ ($M =$ Al, Ga and In) have received significant attention because of their interesting properties, like other iodates, such as non-linear, piezoelectric, pyroelectric and second harmonic generation properties [18–20].

Over the past several years, we have investigated the electrical, calorimetric and thermal properties of some hydrogen-bonded molecules [21–23]. The present work focuses on the electrical properties of the NH_4IO_3 in the polycrystalline form and to discuss the data in the light of different conduction mechanisms. Previous measurements on single crystals showed some discrepancies [7,8–13]. The authors attributed their different results to the conditions of preparation. Our study was originally motivated by the desire to confirm and investigate the improper ferroelectric character of the NH_4IO_3 as proposed by Bismayer *et al.* [12]. Furthermore, we wish also to compare the behaviour of this compound with that of the similar improper ferroelectric KIO_3 [6].

The phenomenon of the ac conductivity dispersion in solids is generally analyzed using the relation [24–28].†

$$\sigma_{\text{tot}}(\omega) = \sigma(0) + \sigma(\omega) \tag{1}$$

where $\sigma(0)$ is the dc conductivity and since $\sigma_{(\omega)} \alpha\ \omega^{s(T)}$ therefore, one may write:

$$\sigma(\omega) = A(T)\omega^{s(T)}. \tag{2}$$

The exponent s ($0 < s < 1$) in the power law represents the degree of interaction between mobile ions with lattices around them. The pre-factor A determines the strength of polarizability [27]. The complex permittivity $\varepsilon^*(\omega)$ is expressed in terms of the real and imaginary parts $\varepsilon'(\omega)$ and $\varepsilon''(\omega)$ respectively as:

$$\varepsilon^*(\omega) = \varepsilon'(\omega) - i\varepsilon''(\omega). \tag{3}$$

2. Experimental

2.1. *Sample preparation*

The material (NH_4IO_3) used in this work was supplied by the BDH Chemical Ltd Company.

†The literature in this field are extensive and hence the refs. [24–28] are only just examples.

To remove the effect of grain size and grain boundary (which are closely related), a suitable amount of the fine polycrystalline of NH_4IO_3, sufficient to prepare 5–6 pellets was further grained under 2 μm (micronized) by ring motor and sieved using a Frituch machine.

A micro analytical balance, type Sartorius, was used to achieve the equality of masses between all samples (before compressing). These samples were pressed under the same pressure, so we have practically identical pellets of ≈2 mm thickness.

Good electrical contact was attained by painting the opposite faces of each pellet with air drying conducting silver paste. Before any measurements, the samples were inserted in a dissector over night to remove any humidity.

The possibility of diffusion of silver paste was controlled by using the electron microscope.

2.2. *Electrical measurements*

The sample is placed in its holder, which is specially designed to fit the present measurements. The temperature of the sample was raised slowly while it was in a specially built electric furnace and its value is recorded by a digital system. A computerized LCR bridge was used to determine the ac conductivity and dielectric permittivity at some selected frequencies. The dc conductivity was measured by using an electrometer, type Keithly 614. Data were collected on at least four virgin samples and the results were found to be quite consistent and reproducible. Most of measurements were performed during the sample being heated. One can conduct heating and cooling runs for demonstrating the existence of thermal hysteresis. The heating rate was $0.5\,K^{-1}\,min^{-1}$ and the experimental error of temperature determination is better than 1%. All measurements were performed at the thermal equilibrium.

2.3. *Ferroelectric hysteresis loops: (D-E) hysteresis loops*

The digital storage oscilloscope (GDS-820S), provided with a computerized camera is connected in the designated electric circuit, the oscilloscope is used to record the loops at different temperatures.

2.4. *Thermal analysis*

The differential scanning calorimetry (DSC) Shimadzu DSC-60 was used to measure the thermogram of the sample, on the other hand the thermo gravitic analysis (TGA) thermogram was recorded by using Shimadzu TGA-50 H at the micro analytical center, Cairo University.

3. Results

3.1. *D-E hysteresis loops*

The ferroelectric hysteresis loops, as displaced on the monitor of the digital oscilloscope at some selected temperatures in ferroelectric and paraelectric phases, are shown in figure 1.

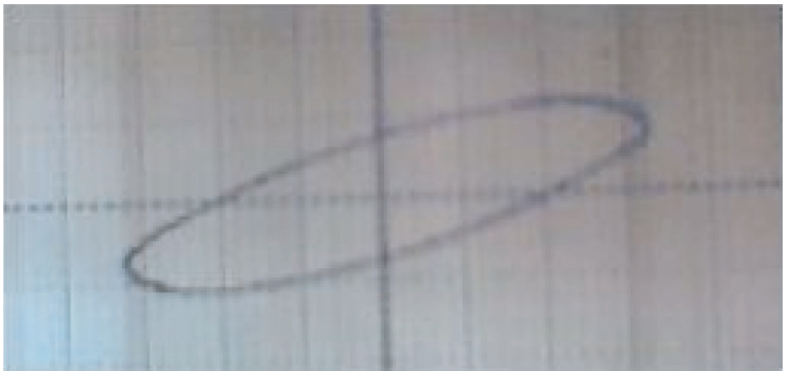

Ferroelectric phase

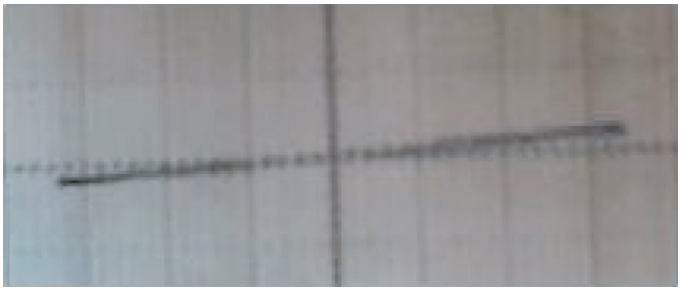

Paraelectric phase

Figure 1. The D-E hysteresis loops in the ferroelectric and paraelectric phases.

It seems likely that the saturation in the D-E loops is quite insufficient. This is also the case for single crystal measurements.

3.2. *Electrical Parameters*

3.2.1. Dielectric permittivity. Figure 2(a) shows the temperature dependence ($300\,\mathrm{K} < T < 400\,\mathrm{K}$) of the real part ε' of the dielectric permittivity ε^* measured at some selected frequencies (1–20 kHz). The behaviour of ε'–T seems to be dependent on both temperature and frequency. In general, and as it is clear from the plot, the value of ε' decreases as the frequency increases over the whole temperature range.

For a given frequency, (say 1 kHz), the value of ε' increases gradually with increasing temperature in the range ($300\,\mathrm{K} < T < 358\,\mathrm{K}$) over a somewhat broad curved path. Beyond a temperature of about 360 K, the rate of increases of ε' with temperature becomes very fast, leading to a peak anomaly in the ε' *versus* T plot centered at (386 ± 1)K. However, beyond a temperature of about 373 K, the value of ε' seems to be almost temperature independent for frequencies ($f \geq 1\,\mathrm{kHz}$).

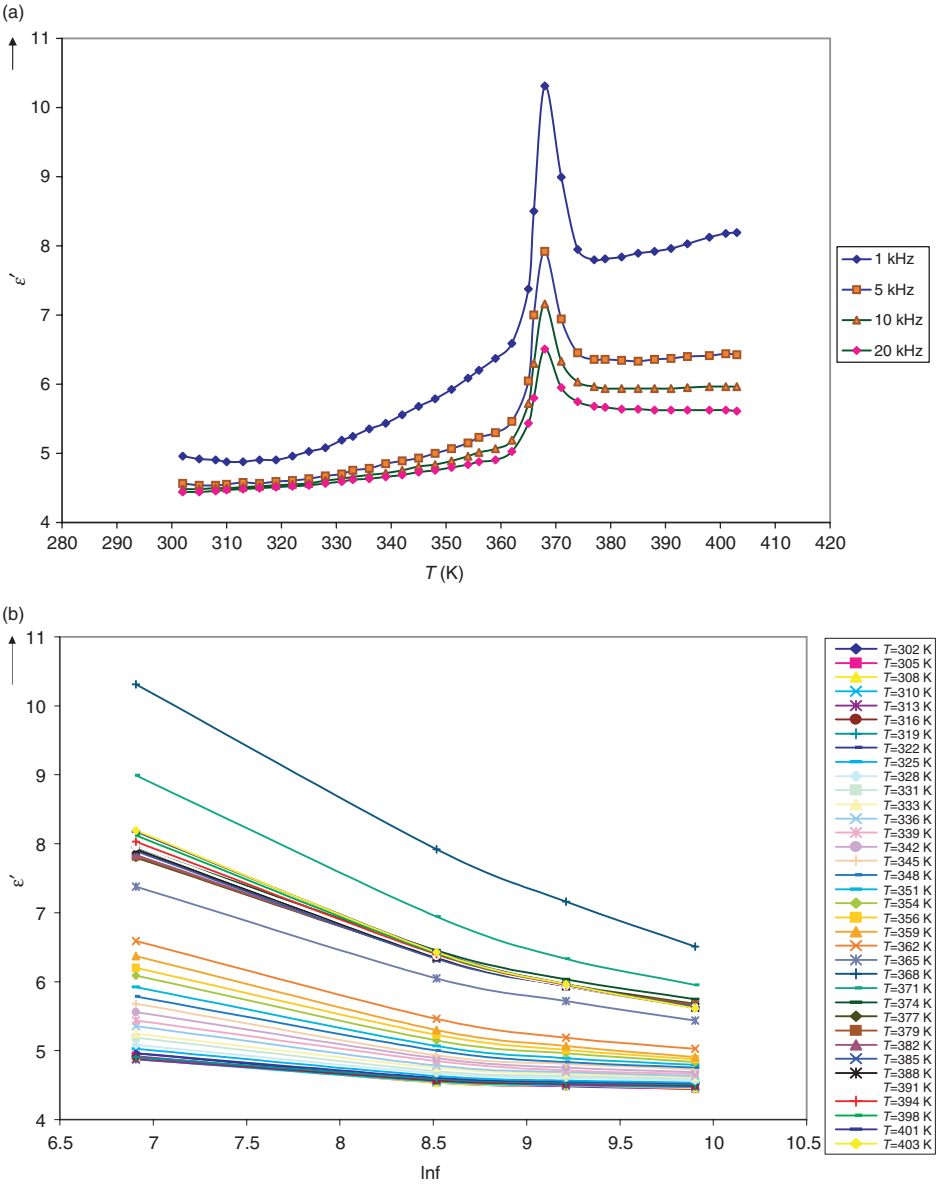

Figure 2. (a) Temperature and frequency dependence of the real part (ε') of the dielectric permittivity. (b) Relation between ε' *vs.* ℓnf at different temperatures.

Thus, the general trend of this plot strongly suggests the existence of a ferroelectric phase transition at the above mentioned temperature (368 ± 1)K. Hence, there are two phases designated by I&II corresponding to the high temperature paraelectric phase and the low temperature ferroelectric phase, respectively.

The frequency dependence of ε' in the temperature range $300\,\mathrm{K} < T < 405\,\mathrm{K}$ is shown in figure 2(b). The dispersion increases with increasing temperature and decreasing frequency in accordance with the typical behaviour of the dielectric.

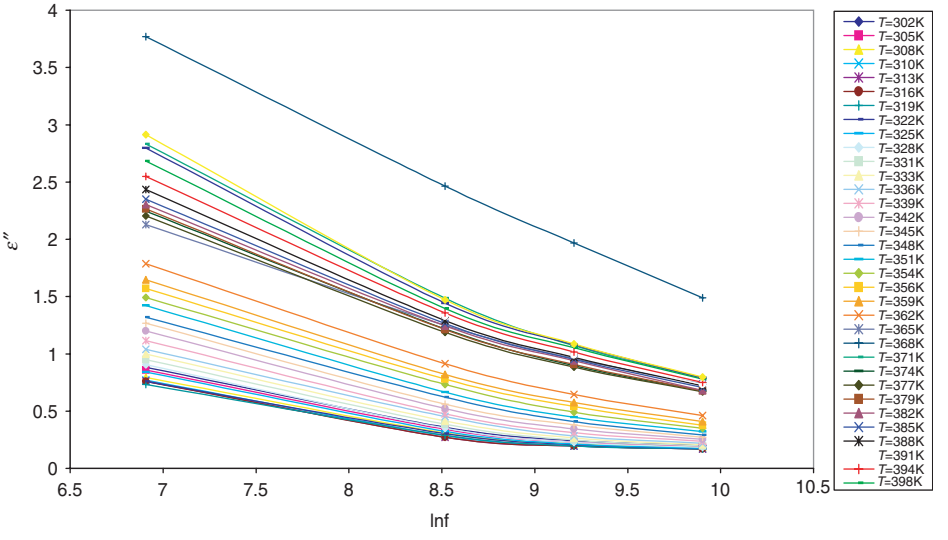

Figure 3. Relation between ε'' *vs.* ℓnf at different temperatures.

The frequency dependence of ε'' is shown in figure (3), where ε'' against (ℓnf) is shown at different temperatures. The general trend of the plot follow the typical behaviour of dielectric, where the dispersion is observed at low-frequency and somewhat high temperature.

3.3. *Electrical conductivity* $\sigma_{(\omega)}$

3.3.1. Temperature dependence. The thermal variation of $\sigma(\omega)$ in the temperature interval $305\,\mathrm{K} < T < 400\,\mathrm{K}$ measured as a function of frequency 5–100 kHz is presented in figure 4 as, ℓn (σT) *versus* $1/T$. It is known that, Arrhenius relation ℓn (σT) α–$E_g(1/T)$ proposed that the mobile ions are thermally activated by E_g. Depending on the temperature range, one can discriminate two regions designated I and II. The two regions are significantly frequency-dependent. ($\sigma_{(\omega)}$ increases with increasing frequency.)

In the low-temperature region, $308\,\mathrm{K} < T < 360\,\mathrm{K}$, which represents the ferroelectric phase II, the activation energy decreases with increasing frequency. At a frequency of 5 kHz, $E_g \simeq 0.256$ eV. In the paraelectric phase or the high-temperature region, the conductivity is very weakly thermally activated and the activation energy is almost independent of the applied frequency [9]. For example, at $f = 5$ kHz, Eg = 0.15 eV.

3.3.2. Frequency dependence. Figure 5 shows the behaviour of the frequency dependence of $\sigma_{(\omega)}$, where a relation between ℓn(σ) against ℓn(ω) is plotted. The graph is characterised by sets of approximately straight lines of different slopes in accordance with the universal dynamic response. The plot shown in figure 5 is known as double ℓn plot. The slope of each line represents the value of s at that temperature.

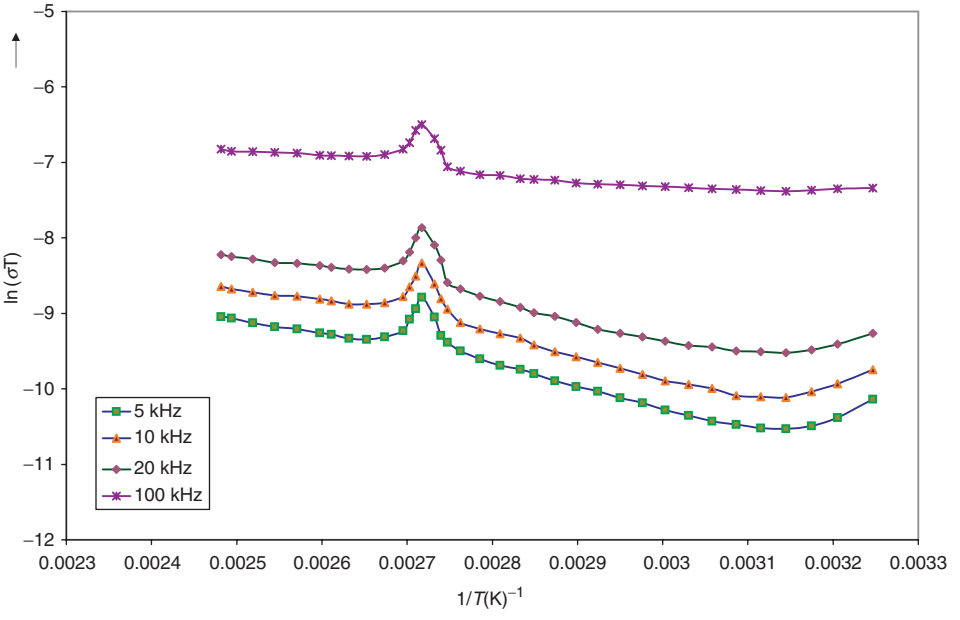

Figure 4. Variation of ($\ln \sigma T$ *vs.* $1/T$) at different temperatures.

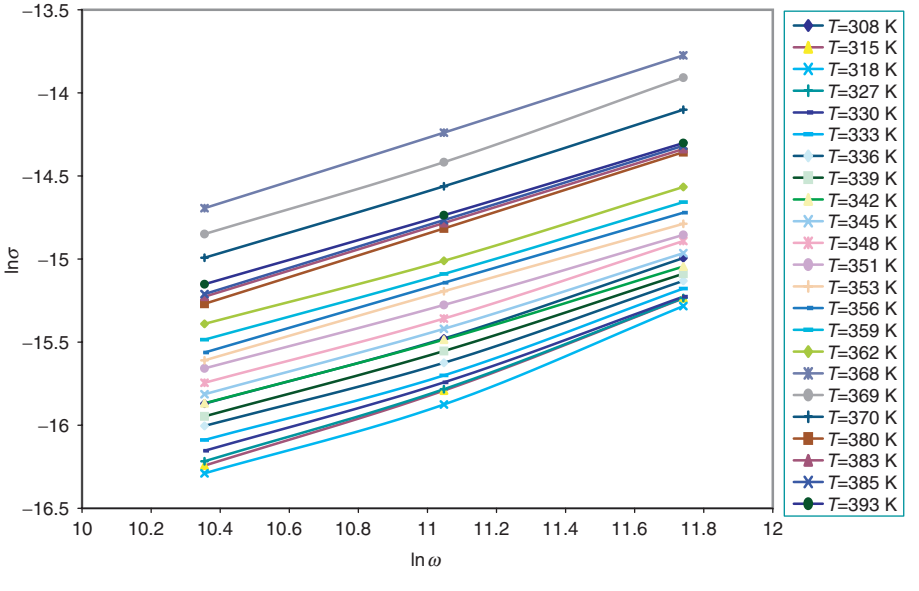

Figure 5. Double logarithmic plot: ($\ln \sigma$ *vs.* $\ell n\omega$).

In figure 6(a), the thermal variation of s is shown. As one can see, the value of *s* decreases with increasing temperature up to ≈362 K, where *s* reaches its minimum value and then starts to increase with increasing temperature and becomes almost temperature independent over the temperature interval (374–400 K).

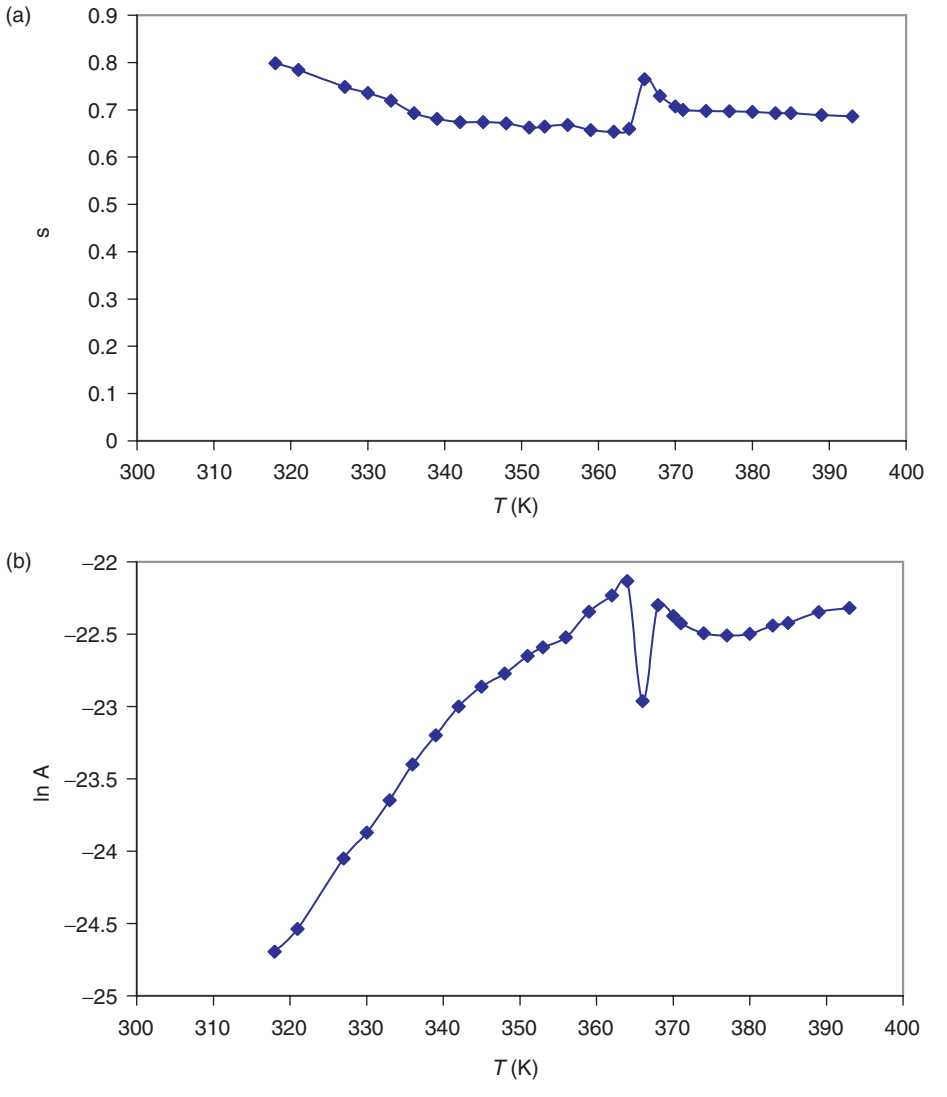

Figure 6. (a) Temperature dependence of the frequency exponent (s). (b) Variation of ln A *vs.* T.

3.4. *Thermal analysis*

3.4.1. Differential scanning calorimetry (DSC). The DSC thermograms at a heating rate of $2^{\circ}C\,min^{-1}$, on heating and cooling runs, are shown in figure 7(a). The thermograms are characterized by an endothermic peak at 91.95°C (364.95 K) on heating, and an exothermic peak at 88.38°C (361.38 K), on cooling. With a thermal hysteresis of 3.57°C.

3.4.2. Thermogravimetric analysis (TGA). The TGA thermogram in the temperature range $315\,K < T < 640\,K$ is shown in figure 7(b). The general feature of this plot

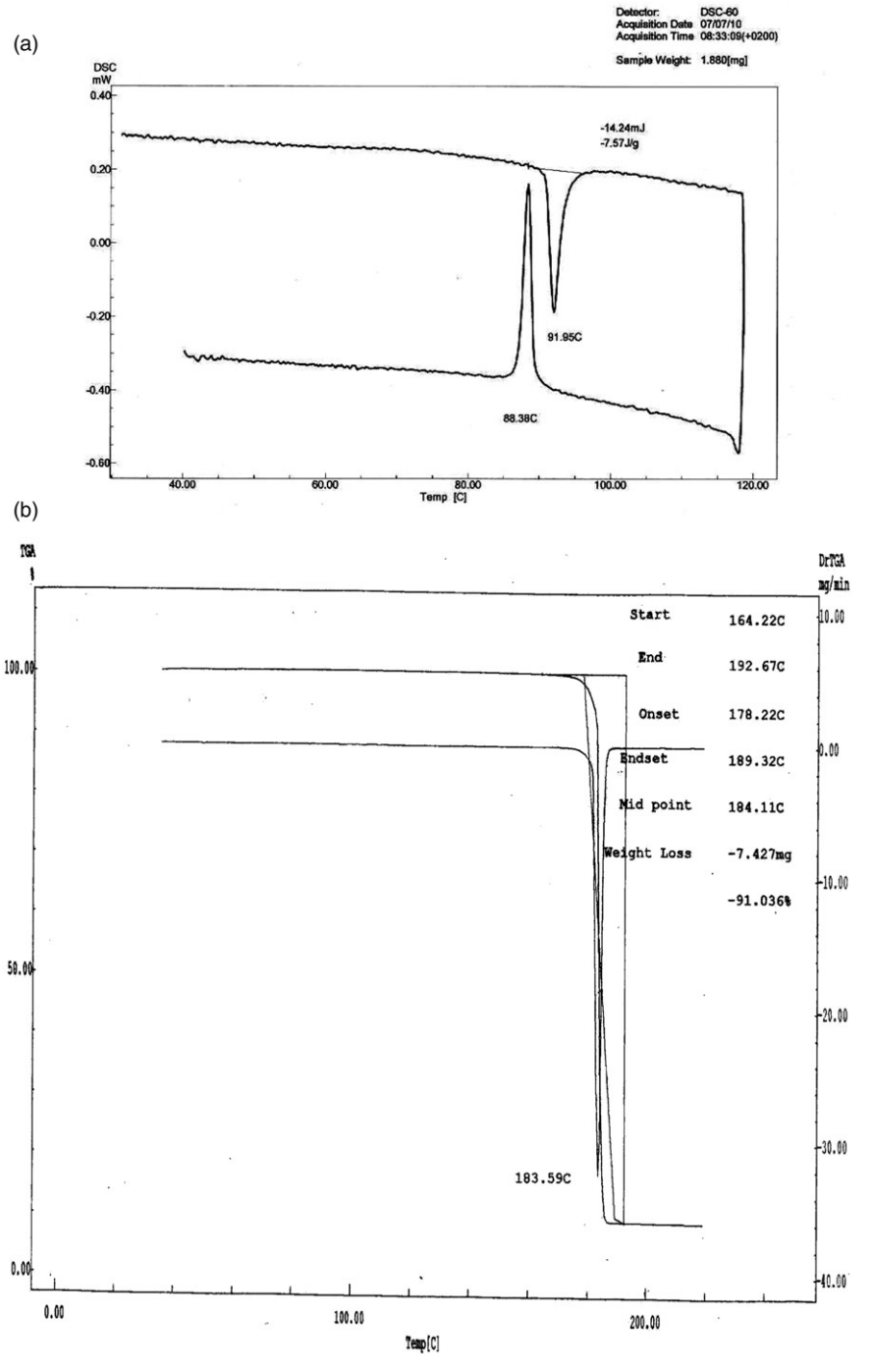

Figure 7. (a) DSC thermogram. (b) TGA thermogram.

is that, there is practically no loss of weight. i.e. no decomposition from the sample. Thus, the endothermic peak that appears at ≈366 K in the DSC thermogram is a reflection of the structural phase transition.

4. Discussion

The electrical parameters presented in this work combined with the behaviour of the (*D*-*E*) hysteresis loops with temperature suggested that, the NH_4IO_3 compound undergoes a ferroelectric phase transition at (368 ± 1)K, from a high temperature paraelectric phase, to a low temperature ferroelectric phase. The value of the mentioned transition temperature is in good agreement with the recent value of Curie temperature Tc ≈ 367 K, obtained from the IR and Raman spectroscopy, in addition to the ^{127}I nuclear quadruple resonance (NQR) spectra of the NH_4IO_3 [14, 15]. Furthermore, regarding the magnitude of ε' at the transition temperature T_c, (figure 2(a)), it seems likely that, the anomaly at Tc is small compared with the usual value of the ferroelectric transitions. At this point, it is of interest to mention that, for the common (proper) ferroelectric transition, the order parameter is the spontaneous polarization and the anomalies in the dielectric properties are the direct consequence of the increased correlation in the order parameter fluctuations near Tc [29]. Obviously, the absence of spike in the ε'-T, figure 2(a) reveals that the transition observed at (368 ± 1)K in the NH_4IO_3 is not of the proper type ferroelectrics. Thus, it is necessary to discuss the second class of ferroelectrics namely, the improper type ferroelectric. For such a transition, the order parameter is not the spontaneous polarization but, for instance, a frozen in zone boundary mode [29]. Among the best known examples of this type are $Gd_2(MoO_4)_3$ "(GMO)" and its isostructural molybdates of Sm, Eu, Tb and Dy. The details are given elsewhere [30, 31]. The transitions are, in general, of the first order.

The conclusion we could arrive at is that, the general feature of the ferroelectric phase transition in the present compound seems to be similar to that of the improper (extrinsic) ferroelectrics. The manifestations of this behaviour are: the small anomaly of ε' near the transition temperature Tc, [present work], the high value of the spontaneous strain [4] and, the thermodynamic order parameter is strongly correlated with the title angles, which are—in the first order perturbation theory—independent of ferroelectric effect. At this point, it is necessary to distinguish between two classes [32].

(i) those where the order parameter η and the spontaneous polarization p_s have different symmetry properties as GMO; (ii) where the η and p_s have the same symmetry as in the KH_2PO_4, where the order parameter is connected with the order of proton in the H-bond, and p_s is connected with the displacement of the lattice ions. It is obvious that the NH_4IO_3 belongs, in general, to the second class and in particular to the KH_2PO_4 improper type ferroelectrics. Although, the two compounds (NH_4IO_3 and KH_2PO_4) are hydrogen-bonded in their crystalline states, yet, they differ in their hydrogen-bonding (H-bond) system. For the KDP, the H-bond is of the short (strong) type, whereas, the H-bond in the NH_4IO_3 belongs to the long (weak) type. When the A−H··· B hydrogen bond is formed, the corresponding potential curve of the proton is modified (figure 8).

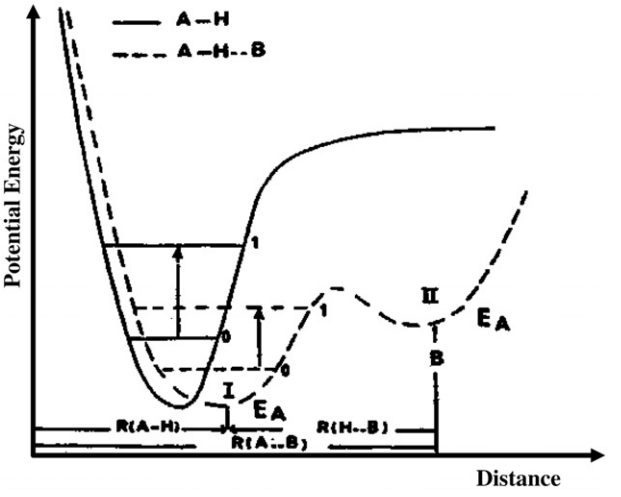

Figure 8. Potential energy of the proton involved in the A–H···B hydrogen bond. (after P. Colomban). Proton Conductors. P. 368.

The phase transition mechanism, in the hydrogen-bonded ferroelectric materials and the origin of the large isotopic effect on the critical temperature, T_c for $H \rightarrow D$ exchange are still a subject of discussion. There are two interpretations. One assumes that, above T_c, protons randomly occupy two positions A—H···B and H···B—A along the hydrogen bond, which results in the order – disorder phase transition mechanisms. The other pre-supposes that such a distribution reflects protonic wave function and hence a tunneling motion in a double well potential of the hydrogen bond (figure 8). A model based on this assumption, the proton tunneling model, predicts a displacive phase transition mechanism. The tunneling model was first suggested by Blinc [33], modified by others [16, 34, 35] and was supported recently using neutron Compton scattering [16]. The properties of the hydrogen-bonded ferroelectrics cannot be explained by one of the two models alone. In recent years, several theories and models such as modified strong dipole-proton coupling (MSDPC) model [36] predict mixed-order – disorder and displacive behaviour of polarization dynamics in the hydrogen bonded ferroelectrics.

It is known that, the ferroelectric phase change represents a special class of structural phase transition denoted by the appearance of spontaneous polarization. Fortunately, the mechanism of such a transition was discussed in the light of the crystal structures and some properties of the NH_4IO_3 [12, 15]. In fact, most of the properties of this compound were investigated by Salje, Viswanathan and Bismayer [9–12].

A model for the structural phase transition to paraelectric phase, was proposed earlier by Viswanathan *et al.* [10], based on rearrangements of the IO_3 pyramids. The next analysis of the β-phase† ($83^\circ C < T < 120^\circ C$) has been supported and confirmed this model [12].

In other words, for the ferroelectric or room tempreature phase, the IO_3 groups can be considered as nonregular IO_3^- pyramids, which are oriented in zig-zag chains

†As designated by author.

along the polar *b*-axis according to the space group $Pc2_1n$. In β-phase, more regular pyramids are formed. Furthermore, there is a displacement of the NH_4^+ along the *b*-axis.

Summarizing the reorientational motion of the IO_3^- and the displacement of the NH_4 are responsible for such a transition.

From the vibrational spectroscopic investigation [15], it is found that, while approaching the phase transition temperature, the IO_3^- ion pseudo-symmetry in the crystal increases from C_1 or C_s to C_{3v}. The spectroscopic investigation also indicated a change in the NH_4^+ ion pseudo-symmetry from C_i in the ferroelectric phase to T_d in paraelectric phase.

In the present work, our vision is that, we cannot neglect the effect of the hydrogen bonding on the structural phase transition. According to the data of ref. [4], in the ferroelectric or the room temperature phase, the IO_3^- and NH_4^+ form chains parallel to the polar axis and there are four N–H–O hydrogen bonds of length between 2.86 up to 3 Å i.e., we have a weak type hydrogen bond.

The weakness of such bonds, with increasing temperature, plays a role in the reorientational motion of IO_3 and hence, the formation of more regular IO_3^- pyramids in the high temperature paraelectric phase I.

Another point of interest is that, according to Barabash *et al.* [15], the phase transition in this compound has the attributes of first order and second order, yet, our data present this work suggest the transition is to be of the first order. A thermal hysteresis of about 3.57°C is observed in the DSC thermogram (figure 7(a)), compared with (3.5 ± 0.5 K) according to spectroscopic data [14] and with 5 K, as it is clear from figure 9(a) and (b), where ε'-T and ρ-T are plotted during heating and cooling runs for two virgin samples in the transition temperature region. (ρ represents the resistivity.)

Regarding the electric conduction, it is known that, in the hydrogen-bonded crystals, the conduction takes place through the proton transfer (migration) along the chain of H-bond. In other words, the electric conduction is essentially protonic. The literature in this field are extensive, examples are: NH_4Cl [37], $NH_4H_2PO_4$ [38] and $NH_4H_2(IO_3)_3$ [39]. There are different mechanisms for proton transport, some of these are solutionic [40], non-linear or one-dimenational model [41] and kink dynamics [42].

Thus, in the present compound a similar situation may also exist i.e., the charge carriers could be protons and hence the motion of protons through the bridge of the H-bond is the main cause of the electric conduction. The similarity is clear between $NH_4H_2(IO_3)_3$ and NH_4IO_3. The two compounds contain the NH_4 and IO_3 groups. Furthermore, they belong to the weak-type H-bond [4, 39]. Although, the present measurements were performed on polycrystalline samples, yet, the obtained activation energy [0.256 eV] lie within the limit [0.1–1.0 eV], which is considered as proton hopping among hydrogen defects [43, 44]. The advantage of measurements on a large single crystal is the ability to investigate the mobility anisotropy, which can not be determined using the polycrystalline technique.

Regarding the behaviour of the temperature dependence of the conductivity (figure 4), and since the unit cell of this compound in the paraelectric phase increases [10], therefore, the distances between ions also increases [15]. Accordingly, the activation energy somewhat decreases compared with that in the ferroelectric phase. This is found to be the case, where the value of E_g in paraelectric phase is 0.15 eV and in ferroelectric phase is 0.256 eV.

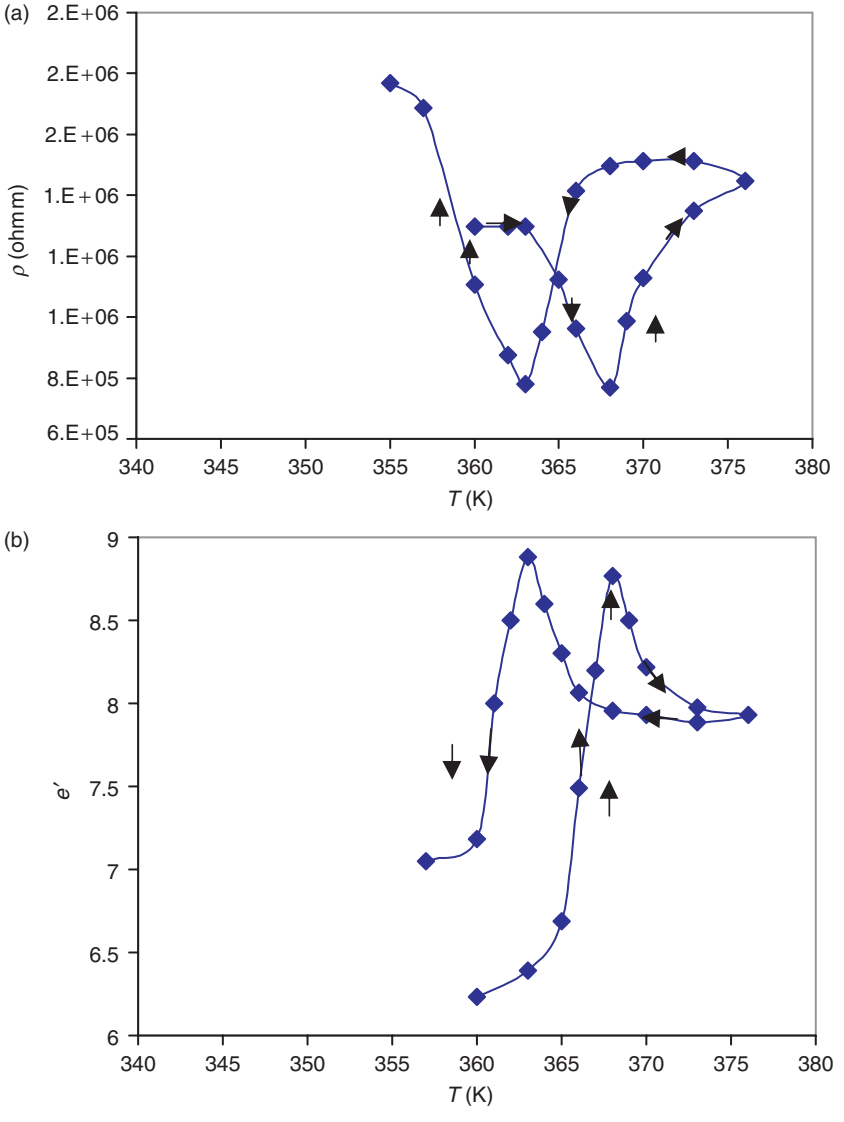

Figure 9. Thermal hysteresis (heating and cooling runs). (a) ε' *vs.* T. (b) ρ *vs.* T.

For the frequency dependent conductivity, figures 5 and 6(a), one can suggest the appropriate model for the conduction mechanism in the light of the theories and models that have been proposed in the literature.

It is known that, there are two distinct processes that have been proposed for the conductivity mechanism, namely quantum mechanical tunneling (QMT) through a barrier and classical hopping over a barrier. The expression for the ac conductivity due to (QMT) is given by [45]

$$\sigma(\omega) = \frac{\pi}{3} e^2 kT[N(E_f)(T)]^2 \alpha - 5\omega \left[\ln\left(\frac{\upsilon_{ph}}{\omega}\right)\right]^4. \quad (4)$$

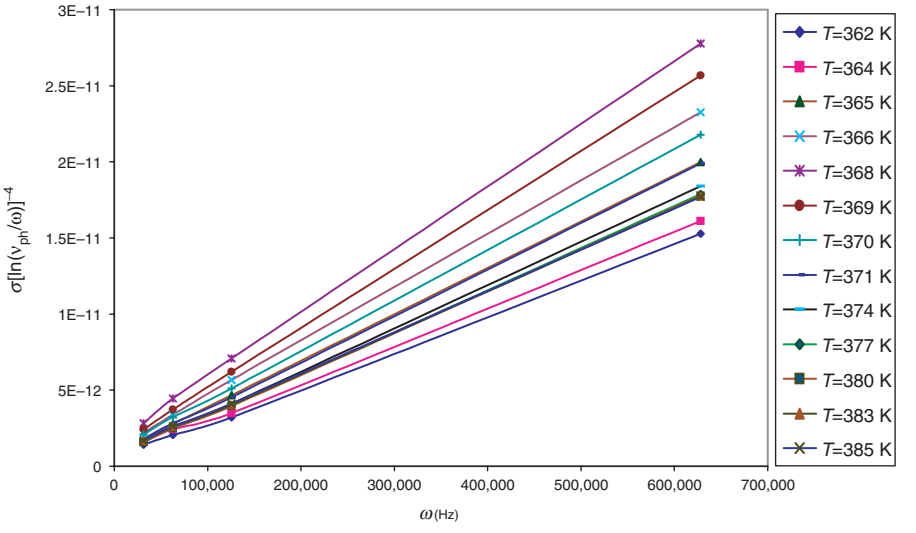

Figure 10. Variation of $\sigma(\omega)/[\ell n(\upsilon_{ph}/\omega)]^4$ *vs.* ω at different temperature.

Where $N(E_f)$ is the density of states at Fermi level, υ_{ph} is the phonon frequency, and is of the order $10^{13}\,\mathrm{sec}^{-1}$ and α is the decay of the localized states wave function ($\alpha \approx 1$ Å).

The last equation predicts a linear relation between $\sigma(\omega)/[\ln(\upsilon_{ph}/\omega)]^4$ and ω.

We have graphically represented our data according to equation (4), in figure 10. The plot shown can be considered as direct evidence that the ac conductivity of this compound behaves in the accordance with equation (4) and therefore, follow the QMT model.

Furthermore, if we substitute with the value of s, $(s = \partial \ln \sigma / \partial \ln \omega)$ into equation (4), one can obtain the expression that describing the behaviour of s, according to this model,

$$s = 1 - \frac{4}{\ell n(\upsilon_{ph}/\omega)}. \tag{5}$$

Equation (5) clearly shows that in case of quantum mechanical tunnelling of the carrier through the potential barrier between sites separated by a distance (R), $(R = 1/2\alpha \ln(\upsilon_{ph}/\omega))$, the value of s should be temperature independent. The plot shown in figure 6(a) strongly supports this conclusion, where s is nearly temperature independent in the range $370\,\mathrm{K} < T < 400\,\mathrm{K}$. i.e. QMT model prevails.

Moreover, if we consider the value of υ_{ph} as $10^{13}\,\mathrm{sec}^{-1}$ and $\omega \approx 10^4\,\mathrm{rad\,sec}^{-1}$, the calculated value of s will be $\approx$0.8, which again, is in a good agreement with the experimental value $\approx$ (0.7) in the temperature range $370\,\mathrm{K} < T < 400\,\mathrm{K}$. Furthermore, the energy spectrum of a proton cannot be considered as a continuum as is usually the case of heavier of particles: i.e., proton energy levels are discrete and their separation is considerable [46]. A thermally activated proton tunnelling can thus frequently be expected.

The behaviour of the ac conductivity seems to be different in the ferroelectric phase II as compared with phase I. this is clear from the same plot figure 6(a), where s decreases with increasing temperature in the range $315\,\mathrm{K} < T < 358\,\mathrm{K}$.

This behaviour agrees quite well with the hopping over the barrier model where s is given by:

$$s = 1 - \frac{6kT}{E_0 - kT\ell n(\upsilon_{ph}/\omega)} = 1 - \frac{6kT}{E_0 - kT\ell n(1/\omega\tau)} \quad (6)$$

Apparently, s is temperature dependent and less dependent on frequency.

Many manifestations of the hopping models and experiments to give value of s in the range of 0.6–1 have been given in the literature [44–48], which is in good agreement with our value of $s \approx (0.80–0.65)$.

Thus, in the mentioned temperature range $315\,K < T < 358\,K$, the hopping over the barrier model is more appropriate than the QMT model. Since, the value of s decreases with the increase of the interaction therefore, the observed minimum in the vicinity of Tc shows a large extent of interaction between charge carriers and the polarization. The relatively higher value of A near Tc (figure 6(b)), is an indication of the presence of higher polarizability.

5. Conclusion

(1) We conducted the first report on the temperature dependence of the ac dielectric permittivity and electrical conductivity of the polycrystalline samples of hydrogen-bonded ferroelectric NH_4IO_3. The measured parameters support each other and indicated the existence of a ferroelectric phase transition of an improper character at $Tc = (386 \pm 1)K$.

(2) It is of interest to compare this transition with that observed in the improper ferroelectric KIO_3 at 487 K. The main difference between them is that, the order parameter η, and the spontaneous polarization p_s, have the same symmetry for NH_4IO_3 and have different symmetry in the case of KIO_3.

(3) Although, the ferroelectric phase transition is mainly displacive, yet, the order–disorder mechanism cannot be excluded. Thus, the transition in general, is ascribed as mixed displacive and order–disorder type.

(4) Depending on the temperature range, there are two types of conduction mechanisms, in phase I the QMT model prevail whereas, the hopping over the barrier model is the most likely one in phase II.

(5) The electric conduction seems to be protonic, where the transport of protons are the main source of energy.

(6) We believe that, the publication of the present work will stimulate more investigations on other parameters such as, geometric isotopic effect and more recent refinement of crystal structure by up-to-date technique i.e., neutron diffraction. Such a recent crystal structure represents the pre-request for any further investigations.

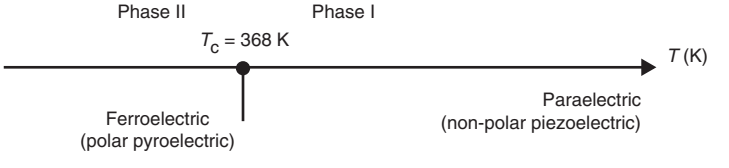

References

[1] S.E. Rogers and A.R. Ubbelohde, Trans. Faraday Soc. **46** 1051 (1950).
[2] M. Okeeffe and C.T. Perrino, J. Phys. Chem. Sol. **28** 211 (1967).
[3] P. Colomban, Proton Conductors, (*Solids, Membranes and Gels Materials and Devices*) *Part I P.1* (Cambridge University Press, Cambridge, 1992).
[4] E.T. Keve, S.C. Abrahams and J.L. Bernstein, J. Chem. Phys. **54** 2556 (1971).
[5] F. Herlach, Helv. Phys. Acta **34** 305 (1961).
[6] M.M. Abdel-Kader, F. El-Kabbany, H. Naguib and W.M. Gamal, Phase Trans. Accepted for publications.
[7] G.R. Crane, J.C. Bergman and A.M. Glass, J. Am. Ceramic Soc. **52** 655 (1969).
[8] T. Oka and T. Mitsui, J. Phys. Soc. Jap **40** 913 (1976).
[9] E. Salje, Acta. Cryst. A **30** 518 (1974).
[10] K. Viswanathan and E. Salje, Acta. Cryst. A **31** 810 (1975).
[11] E. Salje and U. Bismayer, Optics Comm. **20** 303 (1977).
[12] U. Bismayer, E. Salje and K.Viswanathan, Phase Trans. **1** 35 (1979).
[13] H. Shimizu, H. Yamada, N. Yasuda, *et al*., Phys. Stat. Sol. A **51** k121 (1979).
[14] A.I. Barabash, J. Molec. Struc. **508** 81 (1999).
[15] A. Barabash, T. Gavrilko, K. Eshimov, *et al*., J. Molec. Struc. **511** 145 (1999).
[16] G.F. Reiter, J. Mayers and P. Platzman, Phys. Rev. Lett. **89** 23 (2002).
[17] E. Morenzoni, H. Luetkens, A. Suter, *et al*., Physica Rev. B: Condens. Matter **388** 274 (2007).
[18] N. Ngo, K. Kalachnikov, Z. Assefa, *et al*., Sol. Stat. Chem. **179** 3824 (2006).
[19] X. Chen, H. Xue, X. Chang, *et al*., Acta. Cryst. C **61** 1109 (2005).
[20] B. Morosin, J.G. Bergman and G.R. Crane, Acta. Cryst. B **29** 1067 (1973).
[21] M.M. Abdel-Kader, S.E. Gwaily and M.Y. El Zayat, Phys. Stat. Sol. A **19** 49 (2002).
[22] M.M. Abdel-Kader, F. El Kabbany, M.M. Mosaad, *et al*., J. Phys. Chem. Solids **53** 283 (1992).
[23] M.F. Mostafa, M.M. Abdel-Kader and S.S. Arafat, Z. Naturforsch **57** 897 (2002).
[24] A.K. Jonsher, *Dielectric Relaxation in Solids* (Chelsea Dielectric Press, London, 1983), p. 223.
[25] J.C. Dyre and T.B. Schroder, Rev. Mod. Phys. **72** 873 (2000).
[26] S.R. Elliott and A.P. Owens, Phil. Mag. **60** 777 (1989).
[27] C. Karthik and K.B.R. Varma, J. Phys. Chem. Sol. **67** 2437 (2006).
[28] W.K. Lee, J.F. Liu and A.S. Nowick, Phys. Rev. Lett. **67** 1559 (1991).
[29] R. Blinc and B. Zeks, *Soft Modes in Ferroelectrics and Anti Ferroelectrics* (North-Holand Publishing Company, Amsterdam, 1974), p. 2.
[30] M.E. Lines and A.M. Glass, *Principles and Applications of Ferroelectrics and Related Materials* (Oxford University Press, Oxford, 1977), p. 355.
[31] B. Dorner, J.D. Axe and G. Shirane, Phys. Rev. B **6** 1950 (1972).
[32] R. Blinc and B. Zeks, *Soft Modes in Ferroelectrics and AntiFerroelectrics* (North-Holand Publishing Company, Amsterdam, 1974), p. Ch. 10, 45.
[33] R. Blinc, J. Phys. Chem. Sol. **13** 204 (1960).
[34] A. Katrusiak, Phys. Rev. B **51** 589 (1995).
[35] M. Tokunaga and I. Tatsuzaki, Phase Trans. **4** 97 (1984).
[36] D. Merunka and B. Rakvin, Sol. Stat. Comm. **129** 375 (2004).
[37] R.G. Fuller and F.W. Patten, J. Phys. Chem. Sol. **31** 1539 (1970).
[38] M. Sharon and A.K. Kalia, J. Sol. Stat. Chem. **21** 171 (1977).
[39] P. Bordet, J. Boucherle, A. Santoro and M. Marezio, Sol. Stat. Ion. **21** 243 (1986).
[40] A. Gordon, Sol. Stat. Comm. **68** 885 (1988).
[41] S. Pnevmatikos, Phys. Lett. **122** 249 (1987).
[42] A. Gordon, Physica. B **151** 453 (1988).
[43] R.H. Chen, C.-C. Yen, C.S. Shern, *et al*., Sol. State Ion. **177** 2857 (2006).
[44] R.H. Chen, R.Y. Chang, C.S. Shern and T. Fukami, J. Phys. Chem. Sol. **64** 553 (2003).
[45] I.G. Austin and N.F. Mott, Adv. Phys. **18** 41 (1969).
[46] P. Colomban, *Proton Conductors (Solids, Membranes and Gels Materials and Devices)* (Cambridge University Press, Cambridge, 1992), p. 467.
[47] J.C. Dyre, J. Appl. Phys. **64** 2456 (1988).
[48] R.H. Chen, C.S. Shern and T. Fukami, J. Phys. Chem. Sol. **63** 203 (2002).